APPLICATION OF CYCLIC CHRONOPOTENTIOMETRY TO THE STUDY OF SLOW CHARGE TRANSFER REACTIONS AT THE DME AND THE SMDE

Angela MOLINA[1], Joaquin GONZALEZ[2] and Carmen SERNA[3]

Departamento de Quimica-Fisica, Universidad de Murcia, Espinardo 30071 Murcia, Spain; e-mail: [1] amolina@fcu.um.es, [2] josquin@fcu.um.es, [3] cserna@fcu.um.es

Received November 3, 1995
Accepted April 28, 1996

In this work we apply cyclic chronopotentiometry to analyze charge transfer reactions at spherical electrodes, highlighting the influence of electrode curvature and the formation of amalgam on the potential–time response. Moreover, methods are proposed for determining the formal potential and the kinetic parameters of the electrode reaction. Equations obtained for the dropping mercury electrode are transformed to those corresponding to a static mercury drop electrode and a plane electrode.
Key words: Chronopotentiometry; Slow charge transfer reactions; DME; SMDE.

As we have recently demonstrated, the use of a blank period t_{bp} at non-stationary electrodes such as the dropping mercury electrode (DME) offers, among other advantages, the possibility of applying a current step[1]. The application of the cyclic chronopotentiometry at the DME is also possible. In this technique, which can be considered as an extension of current reversal chronopotentiometry[1–4], successive current steps are applied. Their sign is alternately changed at potentials taken at the transition time which corresponds to each potential–time response. This technique is very useful for the evaluation of thermodynamic and kinetic parameters of the reduction and oxidation processes. Until now, however, the theoretical development of this technique has been limited to plane stationary electrodes[5–11].

In this paper we describe an application of cyclic chronopotentiometry in the study of a charge transfer reaction at a DME, considered both as an expanding plane and an expanding sphere. As the general expression deduced for the DME can be applied to other electrodes after simple transformations, static spherical and planar electrodes were considered as well.

The electrode curvature should not be ignored when this technique is used for a DME or a static mercury drop electrode (SMDE). Moreover, we have analyzed the influence of amalgamation on the potential–time response and make possible to determine the amalgam formation from measurements of the transition times. From the results obtained in this paper, cyclic chronopotentiometry has been found to be one of the

best electrochemical techniques for showing both qualitatively and quantitatively the presence of amalgamation.

From the analysis of potential–time curves it is possible to determine the formal potential and the kinetic parameters of the charge transfer reaction.

THEORETICAL

Cyclic chronopotentiometry is a powerful electrochemical technique based on the application of a constant current which is alternately reversed (and its absolute value changed, or not) at potentials taken at the transition times of the various waves, as shown by the Scheme 1 (refs[9–11]),

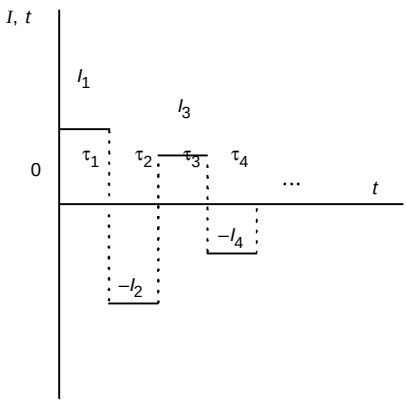

SCHEME 1

where I_j (j = 1, 2,…) is the absolute value of one of the successive current steps applied, and τ_j is the transition time of the process taking place when the j-th is applied.

For the study of a charge transfer reaction

$$\mathrm{A} + n\,\mathrm{e} \underset{k_\mathrm{b}}{\overset{k_\mathrm{f}}{\rightleftharpoons}} \mathrm{B} \qquad (A)$$

by cyclic chronopotentiometry, we have demonstrated in a previous paper that the superposition principle is applicable independently of the geometrical characteristics of the electrode[12]. The expressions for the surface concentrations of species A and B deduced for any current step $(-1)^{j+1}I_j$ with $j \geq 1$ are given by

$$\frac{C_\mathrm{A}^j(r_0,t)}{C_\mathrm{A}^*} = 1 - N_\mathrm{DME} \sum_{m=1}^{j} (-1)^{m+1} (t_{mj})^{1/2} \left(\frac{I_m + I_{m-1}}{I_1} \right) H_{\mathrm{A},m} \qquad (1)$$

$$\frac{C_{\mathrm{B}}^{j}(r_0,t)}{C_{\mathrm{A}}^{*}} = \frac{C_{\mathrm{B}}^{*}}{C_{\mathrm{A}}^{*}} + \gamma N_{\mathrm{DME}} \sum_{m=1}^{j} (-1)^{m+1} (t_{mj})^{1/2} \left(\frac{I_m + I_{m-1}}{I_1} \right) H_{\mathrm{B},m} \ , \qquad (2)$$

where

$$t_{mj} = \sum_{k=m}^{j-1} \tau_k + t_j \quad k < j \qquad (3)$$

$$t_{jj} = t_j \qquad (4)$$

$$I_0 = 0 \qquad (5)$$

$$N_{\mathrm{DME}} = \frac{2I_1}{nFA(t)\sqrt{D_{\mathrm{A}}}C_{\mathrm{A}}^{*}} \qquad (6)$$

$$\gamma = \sqrt{D_{\mathrm{A}}/D_{\mathrm{B}}} \ . \qquad (7)$$

The area of a DME, $A(t)$, is given by Eq. (*8*)

$$A(t) = A_0(t_{\mathrm{bp}} + t)^{2/3} \ , \qquad (8)$$

where t_{bp} is a blank period preceding to the application of the first current step[1]. The time t in Eq. (*8*) refers to the time elapsed between the beginning of the electrolysis and any instant of which the current step is applied, i.e.

$$t = t_{1j} = \tau_1 + \tau_2 + \ldots + t_j \ . \qquad (9)$$

The $H_{i,m}$ series where i is equal either to A or B is given by

$$H_{i,m} = F_0(\beta_m) \mp \xi_{i,m} F_1(\beta_m) + (\xi_{i,m})^2 F_2(\beta_m) \mp \ \ldots \qquad (10)$$

$$\beta_m = \left(\frac{t_{mj}}{t_{bp} + t} \right)^{1/3} \tag{11}$$

$$\xi_{i,m} = \xi_{0,i} \frac{\sqrt{t_{mj}}}{(t_{bp} + t)^{1/3}} \tag{12a}$$

$$\xi_{0,i} = \frac{2\sqrt{D_i}}{a} \tag{12b}$$

$$a = \left(\frac{3 m_{Hg}}{4\pi d} \right)^{1/3} \tag{13}$$

$$F_0(\beta_m) = \frac{1}{\sqrt{\pi}} \left(1 + \frac{1}{9}\beta_m^3 + \frac{7}{270}\beta_m^6 + \frac{4}{567}\beta_m^9 + \frac{11}{5\,832}\beta_m^{12} + \ldots \right) \tag{14a}$$

$$F_1(\beta_m) = \frac{1}{4} \left(1 + \frac{1}{4}\beta_m^3 + \frac{1}{16}\beta_m^6 + \ldots \right) \tag{14b}$$

$$F_2(\beta_m) = \frac{1}{6\sqrt{\pi}} \left(1 + \frac{2}{5}\beta_m^3 + \ldots \right) . \tag{14c}$$

Throughout this paper, the upper sign in any equation refers to a reaction product B (Eq. (*A*)) which is soluble in the electrolyte solution while the lower sign corresponds to a product B dissolved in the amalgam (this is equivalent to change $\xi_{i,m}$ for $-\xi_{i,m}$).

Equations (*1*), (*2*) and (*10*) are simplified in the following particular cases:

Expanding plane electrode (EPE) model for the DME. By making $\xi_{i,m} = 0$ (which is equivalent to supposing the radius of the DME $r_0 \to \infty$), Eq. (*10*) takes the form

$$H_m^{EPE} = F_0(\beta_m) \tag{15}$$

and, therefore, Eqs (*1*) and (*2*) are notably simplified.

Static mercury drop electrode (SMDE). By making $t_{bp} >> t$ or $\beta_m \to 0$, which implies that $A(t) = A_0 t_{bp}^{2/3} = A$, Eqs (*6*) and (*10*) are simplified to

$$N_{SMDE} = \frac{2I_1}{nFA\sqrt{D_A C_A^*}} \tag{16}$$

$$H_{i,m}^{\mathrm{SMDE}} = \frac{1}{\sqrt{\pi}} \mp \frac{1}{4}\xi_{i,m} + \frac{1}{6\sqrt{\pi}}\xi_{i,m}^2 \mp \frac{1}{32}\xi_{i,m}^3 + \ldots =$$

$$= \pm\frac{1}{\xi_{i,m}}\left(1 - \exp\left(\left(\frac{\xi_{i,m}}{2}\right)^2\right)\left(1 \mp \mathrm{erf}\left(\frac{\xi_{i,m}}{2}\right)\right)\right), \qquad (17)$$

where erf (x) is the Gauss error function of x.

Static plane electrode (SPE). By making $\xi_{i,m} = 0$ and $t_{\mathrm{bp}} >> t$ in Eq. (*10*) we obtain

$$H_m^{\mathrm{SPE}} = \frac{1}{\pi^{1/2}} \quad . \qquad (18)$$

In this particular case, our results are identical to those previously deduced by Herman and Bard[5].

The transition times corresponding to each reduction step (τ_j with j = 1, 3, 5, ..) can be deduced by making Eq. (*1*) equal to zero, while those corresponding to each oxidation step (τ_j with j = 2, 4, 6, …), by making Eq. (*2*) equal to zero. So, we deduce for dynamic electrodes (DME with both expanding sphere and expanding plane models)

$$\frac{C_{\mathrm{A}}^* \sqrt{D_{\mathrm{A}}} nFA_0}{2}\left\{t_{\mathrm{bp}} + \tau_1 + \ldots + \tau_j\right\}^{2/3} =$$

$$= \sum_{m=1}^{j} (-1)^{m+1} (\tau_m + \tau_{m+1} + \ldots + \tau_j)^{1/2} (I_m + I_{m-1}) H_{\mathrm{A},m} \qquad (19)$$

for j odd and

$$-\frac{C_{\mathrm{B}}^* \sqrt{D_{\mathrm{B}}} nFA_0}{2}\left\{t_{\mathrm{bp}} + \tau_1 + \ldots + \tau_j\right\}^{2/3} =$$

$$= \sum_{m=1}^{j} (-1)^{m+1} (\tau_m + \tau_{m+1} + \ldots + \tau_j)^{1/2} (I_m + I_{m-1}) H_{\mathrm{B},m} \qquad (20)$$

for j even.

Equations (*19*) and (*20*) are simplified when $I_m = I_{m-1} = ... = I_1$ and in the case of static spherical or planar electrodes ($t_{\mathrm{bp}} >> t$, with $t = \tau_1 + \tau_2 + ... + \tau_j$). Under these conditions, Eqs (*19*) and (*20*) become

$$(-1)^{j+1}\frac{C_i^*\sqrt{D_i}nFA}{2I_1} =$$

$$= (\tau_1 + \ldots + \tau_j)^{1/2}H_{i,1} + 2\sum_{m=2}^{j}(-1)^{m+1}(\tau_m + \tau_{m+1} + \ldots + \tau_j)^{1/2}H_{i,m} \ , \qquad (21)$$

where i = A or B for j odd or even, respectively. Here $H_{i,m}$ is given by Eq. (*17*) for SMDE and by Eq. (*18*) for static plane electrode.

The general expression for the potential–time response corresponding to each current step is now easily obtained by introducing Equations (*1*) and (*2*) in the Butler–Volmer equation. In this way we deduce for the reduction (j odd) and oxidation (j even) processes,

$$\frac{I_j}{nFA(t)k_s}\,e^{\alpha\eta(t)} = \left[C_A^j(r_0,t) - e^{\eta(t)}C_B^j(r_0,t)\right](-1)^{j+1} \qquad (22)$$

with

$$\eta(t) = \frac{nF}{RT}(E(t) - E^0) \ . \qquad (23)$$

RESULTS AND DISCUSSION

Figure 1 shows the variation of the relation τ_j/τ_1 with j (j odd) for reduction processes and of the relation τ_j/τ_2 (j even) for oxidation processes, j being the number of current steps applied, as obtained from Eq. (*21*) for SMDE. The results obtained for a planar electrode (curves *4*) do not differ significantly from those deduced for spherical electrodes of different radii if the reaction product is soluble in the electrolyte solution. Moreover, in this case the values of the ratios τ_j/τ_1 (j odd) or τ_j/τ_2 (j even) remain practically constant. However, when the amalgamation takes place (white points) both ratios increase the faster the higher is the sphericity. Apparently, the relation τ_j/τ_2 (j even) is more advantageous for detection of the amalgamation process since it corresponds to reoxidation of product B and, therefore, depends on its behaviour.

From these results we can conclude that cyclic chronopotentiometry applied to spherical electrodes can be considered as one of the best electrochemical techniques for indicating both qualitatively and quantitatively the presence of amalgamation process due to the ease with which the relation τ_j/τ_2 (j even) can be measured. This relation depends only on the electrode sphericity at I_j/I_{j-1} fixed when $C_B^* = 0$. It is independent

on the other experimental conditions (see Eqs (*20*) or (*21*)), such as the absolute values of the current steps applied, the electrode area and the initial concentration of electroactive species A, C_A^*.

In Figs 2, 3 and 5 we have plotted $E(t) - E^0$ vs t ($t = \tau_1 + \tau_2 + ... + t_j$) in different conditions.

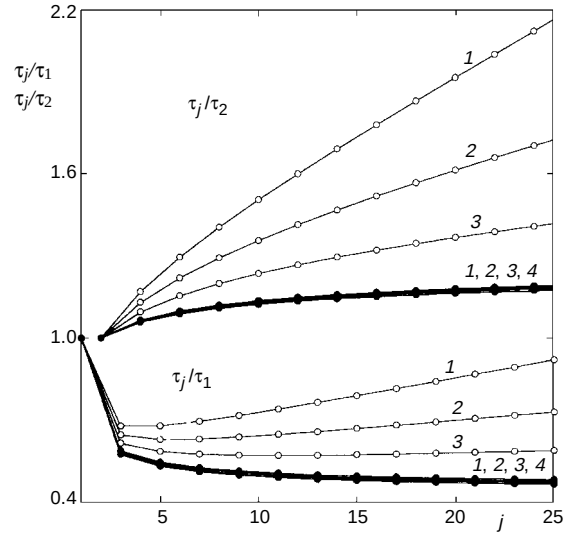

FIG. 1
Influence of the sphericity on the variation of the relative transition times τ_j/τ_1 (j odd) and τ_j/τ_2 (j even) with the number of current steps applied (j) for a SMDE (Eq. (*21*)): ●species B is soluble in the electrolyte solution; ❍ amalgam formation, $I_1 = I_2 = ... = I_{25}$, $C_B^* = 0$, $\gamma = 1$, for values of r_0 (in cm): *1* 0.02, *2* 0.03, *3* 0.06, *4* ∞

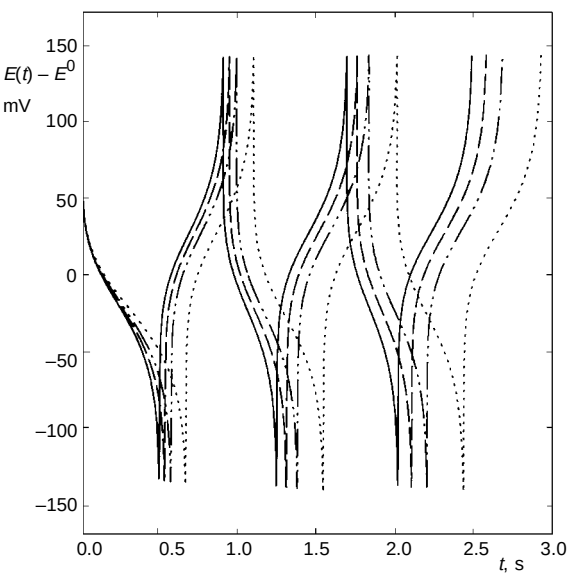

FIG. 2
Electrode curvature effects on the potential–time curves for a reversible process at a SMDE, for both species soluble in the electrolyte solution (Eqs (*1*), (*2*), (*16*), (*17*) and (*22*), $k_s \to \infty$), $N_{SMDE} = 2.5\ s^{-1/2}$, $T = 298$ K, $n = 1$, $D_A = 10^{-5}\ cm^2\ s^{-1}$, $\gamma = 1$, $C_B^* = 0$, $I_1 = I_3 = I_5$, $I_2 = I_4 = I_6 = I_1/2$ and values of r_0 (in cm): ···· 0.015, – ·· – ·· – 0.03, – – – – 0.06 and —— ∞

Figure 2 shows the effect of the electrode curvature on the curves corresponding to a SMDE when the two species are soluble in the electrolyte solution. The effect exerted on these curves by the electrode radius (the sphericity) is very important, and becomes greater with the growing number of current steps applied. Therefore, for the use of this technique at spherical electrodes it is not advisable to neglect the electrode sphericity.

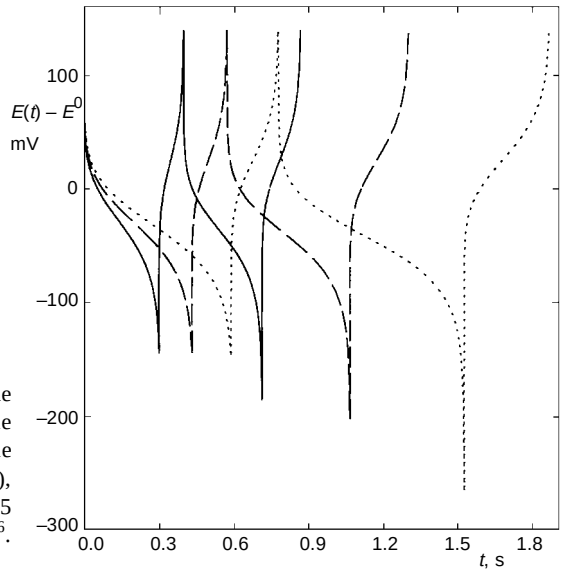

FIG. 3
Influence of the blank period, t_{bp}, on the potential–time curves for a reversible process at a DME, for both species soluble in the electrolyte solution (Eqs (*1*), (*2*), (*6*), (*10*) and (*22*), $k_s \to \infty$), N_{DME} = 3.5 $s^{-1/2}$, $I_1 = I_2 = I_3 = I_4$, $\xi_{0,A}$ = 0.2 $s^{-1/6}$. Other conditions as in Fig. 2

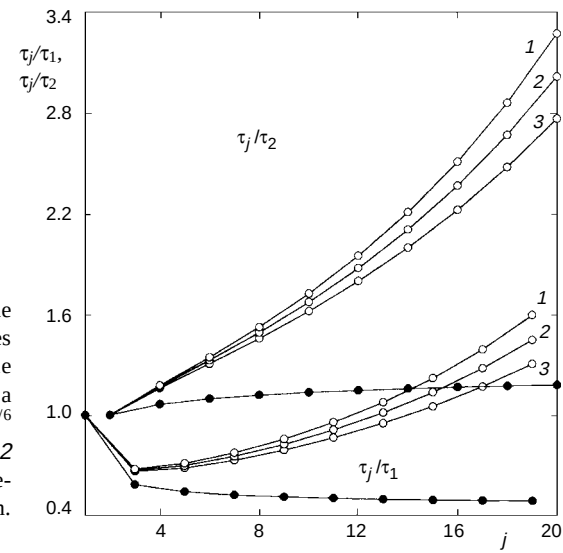

FIG. 4
Influence of the blank period, t_{bp}, on the variation of the relative transition times τ_j/τ_1 (j odd) and τ_j/τ_2 (j even) with the number of current steps applied (j) for a DME (Eqs (*19*) and (*20*), $\xi_{0,A}$ = 0.2 $s^{-1/6}$ and the values of t_{bp} (in s): *1* 1.20, *2* 1.00 and *3* 0.80. The black points correspond to a SMDE with r_0 = 0.03 cm. Other conditions as in Fig. 1

These effects are greater for times near τ_j and become still more important when amalgamation takes place.

In Fig. 3, for a DME, we have plotted the influence of the blank period (t_{bp}), preceding the current step, on the cyclic chronopotentiogram when both species are soluble in the electrolyte solution and $I_1 = I_2 = ... = I_j$. With this electrode, the transition times obtained in the successive steps (especially those of oxidation) increase considerably with respect to those obtained for a static electrode (SMDE). This is due to the decrease of the current density brought about by the electrode growth. To show this, in Fig. 4 we have plotted the variation of τ_j/τ_1 (j odd) and τ_j/τ_2 (j even) with j when both species are soluble in the electrolyte solution for SMDE (black points) and for DME (white points).

The *E/t* curves in Fig. 5 show the effects of amalgamation and reversibility of the electrochemical reaction at SMDE of $r_0 = 0.015$ cm for a reversible (Fig. 5a) and a totally irreversible (Fig. 5b) process. The first reduction curve is affected by the amalgamation very little and no influence was observed for a totally irreversible process, with τ_1 being insensitive to the behaviour of B (ref.[1]). However, these effects increase with the electrode sphericity and the number of alternating current steps applied. Therefore, when amalgamation takes place, the variant of Eq. (*17*) with the lower sign can be used since, in the contrary case, the errors become enormous. By comparing Figs 5a and 5b, it is evident that the process can be classified as reversible or totally irreversible by a mere visual inspection of these curves.

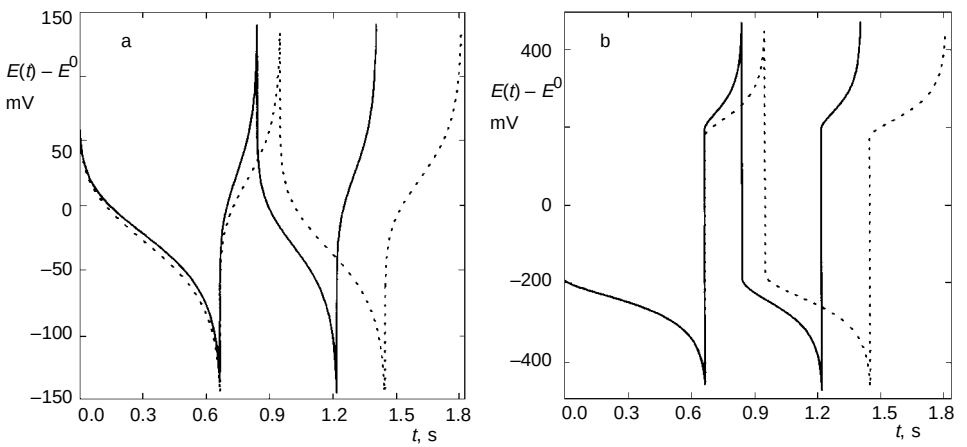

FIG. 5

Influence of reversibility on the potential–time curves at a SMDE (Eqs (*1*), (*2*), (*16*), (*17*) and (*22*)); —— both species are soluble in the electrolyte solution, · · · · amalgam formation, $N_{SMDE} = 2.5\ s^{-1/2}$, $I_1 = I_2 = I_3 = I_4$, $r_0 = 0.015$ cm, **a** reversible process ($k_s \to \infty$), **b** irreversible process with $k_s = 10^{-4}$ cm s^{-1} and $\alpha = 0.5$. Other conditions as in Fig. 2

Moreover, for a totally irreversible process ($k_s \leq 10^{-3}$ cm s^{-1}) it is possible to deduce accurate values of thermodynamic and kinetic parameters (E^0, α and k_s) from analysis of both cathodic and anodic responses. So, from the general Eq. (*22*) for $I_1 = I_2 = \ldots = I_j$ we deduce the following expressions

$$E(t) = E^0 + \frac{RT}{\alpha nF} \ln \frac{nFA_0 C_A^* k_s}{I_j} + \frac{RT}{\alpha nF} \ln g_j^c \quad , \tag{24a}$$

where

$$g_j^c = (t_{bp} + t)^{2/3} \left[1 - N_{DME} \left(t_{1j}^{1/2} H_{A,1} + 2 \sum_{m=2}^{j} (-1)^{m+1} (t_{mj})^{1/2} H_{A,m} \right) \right] \tag{24b}$$

for the cathodic *E/t* responses with $j = 1, 3, 5, \ldots$, and

$$E(t) = E^0 - \frac{RT}{(1-\alpha)nF} \ln \frac{nFA_0 C_A^* k_s}{I_j} - \frac{RT}{(1-\alpha)nF} \ln g_j^a \quad , \tag{25a}$$

where

$$g_j^a = (t_{bp} + t)^{2/3} \left[\frac{C_B^*}{C_A^*} + \gamma N_{DME} \left(t_{1j}^{1/2} H_{B,1} + 2 \sum_{m=2}^{j} (-1)^{m+1} (t_{mj})^{1/2} H_{B,m} \right) \right] \tag{25b}$$

for the anodic ones ($j = 2, 4, 6, \ldots$).

Indeed, by carrying out a linear regression analysis of $E(t)$ vs $\ln g_j^c$ (Eq. (*24*)) or $\ln g_j^a$ (Eq. (*25*)) it is evident that for the particular case $I_1 = I_2 = \ldots = I_j$, the straight lines corresponding to the reduction process as well as those corresponding to oxidation ones are coincident. This particularity allows us to characterize the electrode process (Eq. (*A*)). So, from Eqs (*24*) and (*25*) we deduce following expressions

$$P_{j-1}^c = \frac{RT}{\alpha nF} \quad , \quad P_j^a = \frac{RT}{(1-\alpha)nF} \tag{26}$$

$$\ln k_s = \frac{RT}{nF} \left[\frac{O_j^a - O_{j-1}^c}{P_j^a P_{j-1}^c} \right] + \ln \frac{I_j}{nFA_0 C_A^*} \tag{27}$$

$$E^0 = \frac{P_j^a O_{j-1}^c - P_{j-1}^c O_j^a}{P_j^a - P_{j-1}^c} \qquad (28)$$

for any j even.

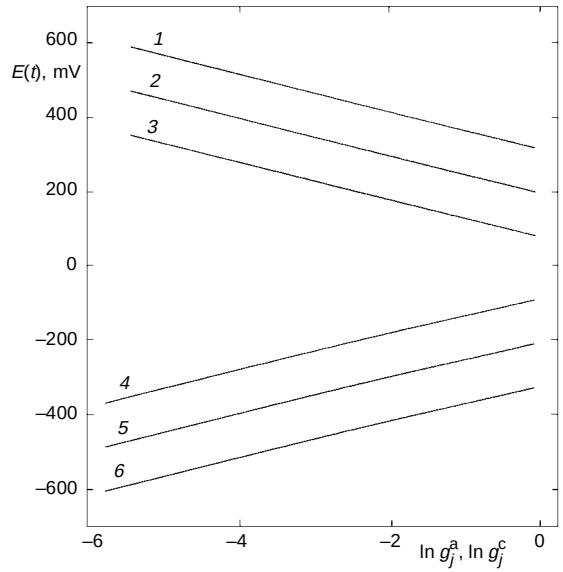

FIG. 6
Dependence of $E(t)$ on g_j^c (Eq. (*24*)) and g_j^a (Eq. (*25*)) for a SMDE, N_{SMDE} = 3.0 $s^{-1/2}$, $I_1 = I_2 = \ldots = I_6$, r_0 = 0.06 cm, α = 0.5. The values of k_s (cm s^{-1}) : 10^{-5} (*1,6*), 10^{-4} (*2,5*), 10^{-3} (*3,4*); current steps j: even (*1–3*), odd (*4–6*). Other conditions as in Fig. 2

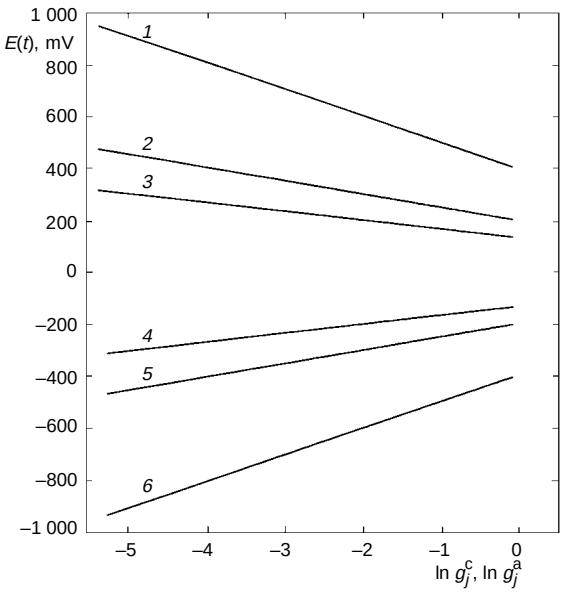

FIG. 7
Dependence of $E(t)$ on g_j^c (Eq. (*24*)) and g_j^a (Eq. (*25*)) for *a* SMDE, $k_s = 10^{-4}$ cm s^{-1}. The values of α: 0.75 (*1,4*), 0.50 (*2,5*), 0.25 (*3,6*); current steps j: even (*1–3*), odd (*4–6*). Other conditions as in Fig. 6

By this method, we obtain α and $(1 - \alpha)$ independently from the slopes of the cathodic and anodic processes, respectively. If there are kinetic complications in any of those processes (consecutive electrochemical reactions, dismutations, etc.) the sum of $\alpha + (1 - \alpha)$ will be different from unity, and such complications can therefore be detected.

As an example, in Figs 6 and 7 we have plotted $E(t)$ vs ln g_j^c and ln g_j^a for $j = 6$ and $I_1 = I_2 = \ldots = I_6$. Figure 6 shows the influence of k_s on these plots, while in Fig. 7 we have considered the influence of the transfer coefficient α.

SYMBOLS

a	radius of DME for $(t_{bp} + t) = 1$ s, $a = (3m_{Hg}/4\pi d)^{1/3}$
A	electrode area, $A = A_0 t_{bp}^{2/3}$, for $t_{bp} >> t$ (static spherical or planar electrodes)
A_0	$(4\pi)^{2/3}(3m_{Hg}/d)^{2/3}$ in $s^{-2/3}$
$A(t)$	time-dependent electrode area (DME), $A(t) = A_0(t_{bp} + t)^{2/3}$
C_A^*, C_B^*	initial concentrations of species A and B
$C_i^j(r_0,t)$	surface concentration of species i, with i equal either to A or B, for the j-th current step
d	density of mercury
D_i	diffusion coefficient of species i
E^0	formal standard potential of electroactive couple
$E(t)$	time dependent potential
I_j	absolute value of the j-th step current
k_f, k_b	heterogeneous rate constants of reduction and oxidation processes, respectively
k_s	apparent heterogeneous rate constant of charge transfer at E^0
m_{Hg}	rate of flow of mercury
r_0	electrode radius at time $t_{bp} + t$ for a DME, $r_0 = a(t_{bp} + t)^{1/3}$, or r_0 is constant for a SMDE
t	time elapsed between application of the first and the j-th current step, $t = \tau_1 + \ldots + \tau_{j-1} + t_j$
t_{bp}	blank period used only for DME
t_j	time during which the j-th current step is applied $(0 \le t_j < \tau_j)$
α	electron transfer coefficient
γ	$(D_A/D_B)^{1/2}$
τ_j	transition time of the j-th step in which a change in sign of the current takes place. If j is odd, τ_j corresponds to a reduction process, whereas if j is even, τ_j corresponds to an oxidation one

Other variables and abbreviations have their usual meanings.

The authors greatly appreciate financial support by the Direccion General de Investigacion Cientifica y Tecnica (Project No. PB93-1134) and DREUCA de la Region de Murcia (Project No. PIB94/73). We would also like to express our gratitude to the reviewer, who has greatly helped us to improve this paper.

REFERENCES

1. Molina A., Albaladejo J.: J. Electroanal. Chem. *256*, 33 (1988); Molina A., Serna C., Lopez-Tenes M.: J. Electroanal. Chem. *278*, 21 (1990).
2. Delahay P., Berzins T.: J. Am. Chem. Soc. *75*, 2486 (1953).
3. Dracka O.: Collect. Czech. Chem. Commun. *25*, 338 (1960); *26*, 2144 (1961); *32*, 3987 (1967); *38*, 1104 (1973); *39*, 805 (1974); *41*, 498 (1976); *41*, 953 (1976); *42*, 1093 (1977).
4. Dracka O., Fischer O.: J. Electroanal. Chem. *75*, 301 (1977).
5. Herman H. B., Bard A. J.: Anal. Chem. *35*, 1121 (1963).
6. Cukman D., Pradic V.: J. Electroanal. Chem. *49*, 415 (1974).
7. Cukman D., Vukovic M., Pradic V.: J. Electroanal. Chem. *49*, 421 (1974).
8. Vukovic M., Cukman D., Pradic V.: J. Electroanal. Chem. *54*, 209 (1974).
9. Bard A. J., Faulkner L. R.: *Electrochemical Methods*, Chap. 5. Wiley, New York 1980.
10. McDonald D. D.: *Transient Techniques in Electrochemistry*, Chap. 3. Plenum Press, New York 1977.
11. Galus Z.: *Fundamentals of Electrochemical Analysis*, 2nd ed, Chaps 17 and 18. Ellis Horwood, Chichester 1994; and references therein.
12. Molina A., Gonzales J., Serna C., Camacho L.: J. Math. Chem., in press.